

EFFECTS OF MODELING ASSUMPTIONS ON THE ACCURACY OF SPECTRUM FATIGUE LIFETIME PREDICTIONS FOR A FIBERGLASS LAMINATE

Neil Wahl
Montana Tech of The University of Montana
Butte, Montana 59701

Daniel Samborsky
John Mandell
Douglas Cairns
Montana State University
Bozeman, Montana 59717

ABSTRACT

This paper will present an extension of the work described in Reference 1, presented at this symposium in 2000, which dealt only with tensile fatigue loads spectra. Experimental results and modeling have now been extended to simple spectra which cover a full range of loads including compression and reversed tension-compression, as well as WISPERX and other spectra representative of wind turbines, containing a full range of R-values. Experimental fatigue data (over 1100 tests) have been generated for a fiberglass laminate which is typical of wind turbine blade construction, tested under a variety loads spectra. Constant amplitude data typical of the DOE/MSU fatigue database are then used with various modeling schemes to predict the lifetime under spectrum loading.

Several areas of current concern in blade lifetime prediction are explored. First, it is demonstrated that the Miner's Rule cumulative damage law results in significantly non-conservative lifetime predictions for most loads spectra. Linear and nonlinear residual strength models are easily applied and are more accurate in predicting lifetime; they also provide a prediction of remaining strength as a function of the history of loading prior to failure. Prediction accuracy is also sensitive to the model (exponential or power law) used to represent and extrapolate the constant amplitude S-N fatigue data. A power law representation appears to provide more accurate predictions of lifetime under spectral loading for longer lifetime cases. The study also explores the methodology used to represent and interpolate the constant amplitude data on a Goodman Diagram.

This research was supported by Sandia National Laboratories under subcontract BC7159.

Copyright © 2002 by the American Institute of Aeronautics and Astronautics, Inc. and the American Society of Mechanical Engineers. All rights reserved.

INTRODUCTION

An investigation into the relationship between spectrum loading and fatigue lifetimes of a fiberglass laminate typical of that used in wind turbine construction was continued. The previous report included fatigue of laminates subjected to loads that were only tensile; this paper includes fatigue under loads that contain compressive and reversing loads as well.

The general testing program progressed from simple constant amplitude loading spectra to multi-block spectra and finally to spectra, which were random in nature such as the WISPERX^{2,3} spectrum.

Once this baseline data were collected, lifetime predictions based upon Miner's rule and rules based upon residual strength degradation were employed and compared to actual lifetimes. Residual strength testing revealed the nonlinear trend of strength versus cycles; with error analysis leading to a nonlinear parameter consistent with that determined by tuning of this parameter to the two-block fatigue data. The nonlinear degradation parameter presented in the earlier report¹ was determined by repeated adjustment until the general trend of prediction lifetimes for two-block spectra matched the actual data. Subsequent to this tuning, error analyses of residual strength calculations and actual strengths led to a similar value for the nonlinear parameter.

All subsequent nonlinear residual strength degradation lifetime predictions were made using this value for the nonlinear parameter. This is true for the all multi-block, modified WISPERX spectra and the unmodified WISPERX spectrum.

Constant amplitude fatigue data were collected and summarized in both S-N and Goodman Diagrams based upon two regression trends, exponential and power law. The prediction accuracy was considered as a function of the number of cycles and either the exponential or power law constant amplitude fatigue trend.

In the application of the residual strength degradation lifetime predictions, the transition of the failure mode from tension dominated to compression became

critical. Estimates of this transition were made based upon the relative ratio of the applied maximum (or minimum) stress to the ultimate tensile (or compressive) strength. The greater of these values was used to determine the selection of the residual strength degradation trend.

NOMENCLATURE AND DEFINITIONS

Miner’s rule⁴ is widely used as a method of lifetime prediction for laminates. Miner’s sum is used to document the actual lifetimes⁵⁻¹⁰

$$Miner's\ Sum = D = \sum_i \frac{n_i}{N_i} \quad (1)$$

where D = damage accumulation parameter
 n_i = number of cycles experienced at σ_i
 N_i = number of cycles to failure at σ_i
 σ_i = cycle’s maximum stress level

Miner’s rule of lifetime prediction is based upon the premise that failure occurs when D, Miner’s sum, reaches unity. Actual Miner’s sum may be greater than or less than 1, depending upon the load spectrum.

Regression analyses of the constant amplitude fatigue data shown in S-N (stress-cycle) diagrams, typically takes on either an exponential (equation 2) or power law (equation 3) form^{5, 11}

$$\frac{S}{S_0} = C_1 - b * \log(N) \quad (2)$$

$$\frac{S}{S_0} = C_2 * N^{(-1/m)} \quad (3)$$

where σ is the applied maximum stress, MPa
 σ_0 is the ultimate strength, MPa
 N is the number of cycles to failure at stress σ
 b and m are regression constants representative of the trend of the fatigue
 C₁ and C₂ are regression constants

The residual or remaining strength¹²⁻¹⁴, of a laminate or component decreases with fatigue cycles. The trend of this decrease may be a function of several parameters, but generally can be described as a generic equation

$$S_R = S_0 + (S_i - S_0) * \left(\frac{n}{N}\right)^{\eta} \quad (4)$$

where σ_R is the residual strength, MPa
 σ_0 is the ultimate strength, MPa
 σ_i is the applied stress, MPa
 n is the number of cycles experienced
 N is the number of cycles to failure at σ_i
 η is the nonlinear degradation parameter

A value of η less than 1 is typical of a material that exhibits a greater loss of strength in the early stages of fatigue; conversely, a value greater than 1 would be the characteristics of a material that has little loss of strength in the early stages of life, but a large loss at the final stages of life. A value of $\eta = 1$ would represent the linear loss of strength with fatigue cycles.

Modifications were made to the published WISPERX spectrum for the purpose of avoiding both complex failure mode interactions and the need to interpolate between different R-values in the Goodman Diagram¹. Mod 2 spectrum was created by forcing the minimum value of each cycle to 10 percent of the cycle’s maximum value. (The unmodified spectrum was also tested.)

Each cycle of loading is typically described by documenting the maximum stress level and an R-value.

$$R - value = \frac{S_{min}}{S_{max}} \quad (5)$$

where σ_{min} = minimum cyclic stress value
 σ_{max} = maximum cyclic stress value

Several common sinusoidal loading waveforms are shown in Figure 1, along with their R-values as well as the general loading regimes.

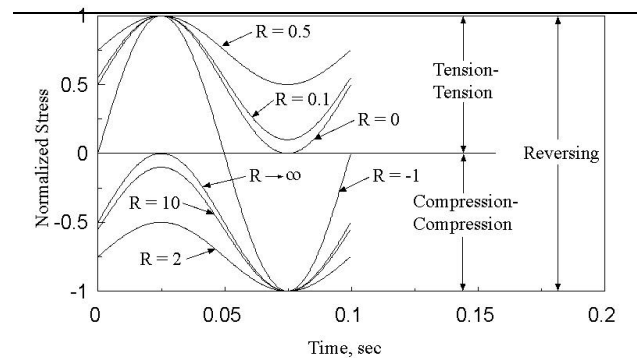


Figure 1. Load Regimes and R-Values

EXPERIMENTAL METHODS

Laminate Material and Test Specimens

The laminate tested during this research was described in References 1, 15 and 16, the laminate is designated DD16 in the DOE/MSU Fatigue Database. Recapping, the chosen laminate was typical of those used in wind turbine blade construction and was comprised of E-glass and polyester matrix in a lay-up of [90/0/±45/0]_S, with a fiber volume fraction of 0.36. Plates which were manufactured by the resin transfer molding process, were cut into coupons of the geometries shown in Figure 2. The 90° surface plies were present to mitigate grip effects.

Coupons were designed for the specific type of test, whether used in tension-tension, compression-compression or reversing load regimes. The tension-tension and reversing coupons were dogbone shaped and were fabricated with fiberglass tabs at both ends. The G10 fiberglass tabs, manufactured by the International Paper Co., Inc., were added to distribute the grip forces, hence reducing grip effects. The tabs of the reversing coupons were longer to aid in reducing elastic buckling by providing lateral support and a shorter gage section. The compression-compression coupons were straight and without tabs. The compression tests were generally run at lower maximum stress levels, consequently, lower hydraulic grip pressures were required.

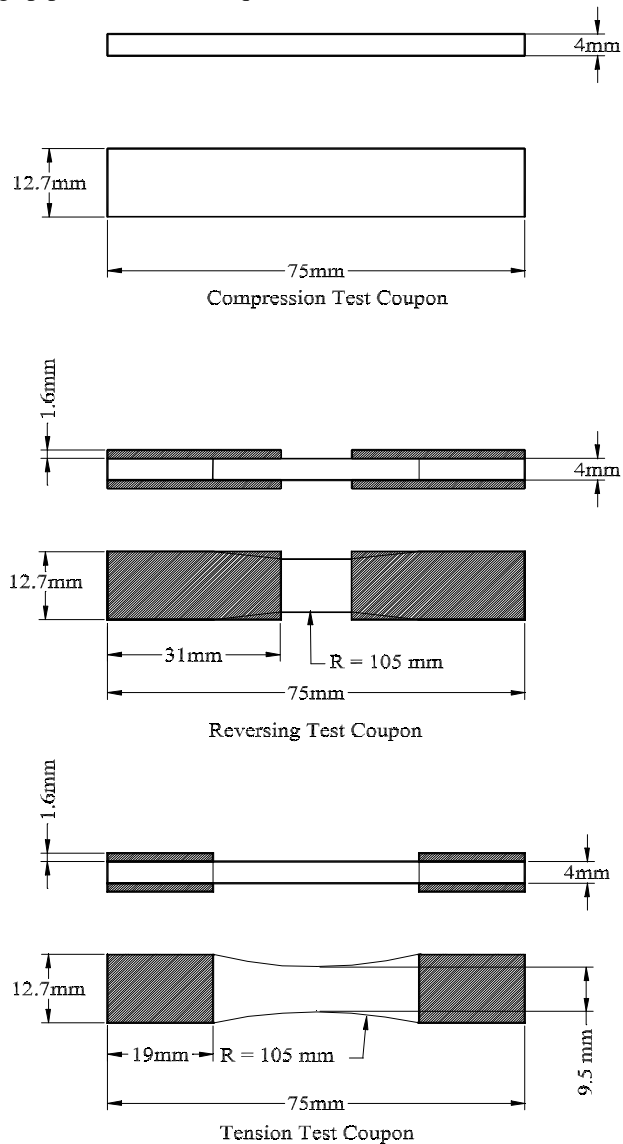


Figure 2. Laminate Test Coupon Configurations

Small Strand High Cycle Specimens

The trend of high cycle extrapolations is important

to predictions of spectrum loading lifetime. Recent results have become available for small strands, tested to 10^{10} cycles; these results are summarized here to clarify the issue of exponential or power law (Equations 2 or 3) data representations.

High frequency / high cycle coupons consisting of 45 E-glass fibers were fabricated from an Owens Corning 990-BC-2385-4093 roving and impregnated with a polyester matrix. Details of these coupons and testing can be found in Reference 15. These small strand tests provided an extension to test results currently listed in the DOE/MSU database which involved larger, 2000 fiber strands, but with cycles only out to the 10^8 to 10^9 range.

Laminate Testing Equipment

Instron 8501 and 8872 mechanical testing machines were used to conduct the ultimate strength and fatigue tests, respectively. Instron 8800 controllers along with Instron's RANDOM[®] software loaded on a PC, were used to apply the loading waveform to the testing machines. Testing was performed at 10 Hz and lower, with forced air surface cooling of the specimen to preclude thermal effects.

Small Strand Testing

Testing equipment (Figure 3) was developed to relatively quickly reach high cycle (10^{10}) fatigue. These machines, which are detailed in Reference 15, were constructed using audio speakers, powered by an 120 watt amplifier and controlled by an Instron 8500 controller. The maximum load was less than 15 N and frequency capability was over 250 Hz. Most long duration tests were operated at a frequency of 200 Hz.

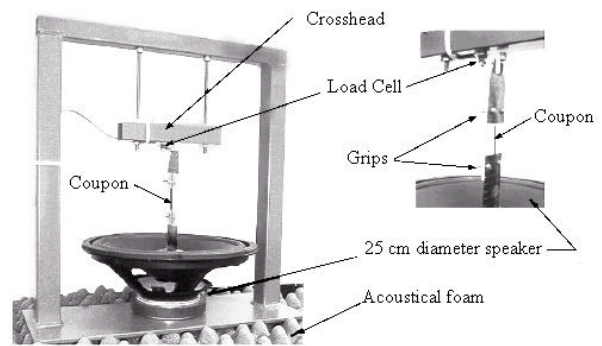


Figure 3. High Frequency Strand Testing Apparatus

TESTING AND RESULTS

Laminate Constant Amplitude Testing

Laminate coupons were tested at R-values of 0.1, 0.5, -1, 10 and 2 to reasonably cover the various load

regimes. The constant amplitude fatigue test results are summarized in the exponential and power law S-N diagrams of Figures 4 and 5, respectively. The regression constants for the curves (Equations 2 and 3) of these two figures are shown in Table 1, along with the ultimate strengths. These are typical of the constants reported in Reference 5 for unidirectional laminates. The trend is asymmetrical over the tension to compression regions of loading.

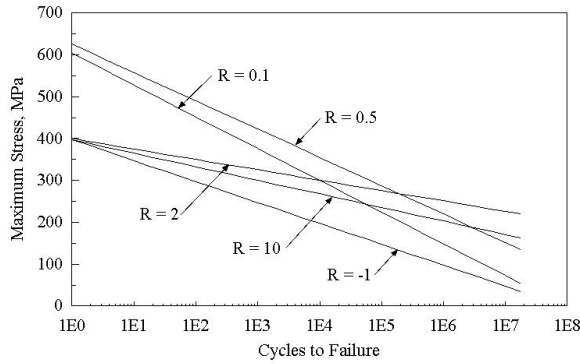


Figure 4. Laminate Constant Amplitude S-N Diagram Exponential Fatigue Models

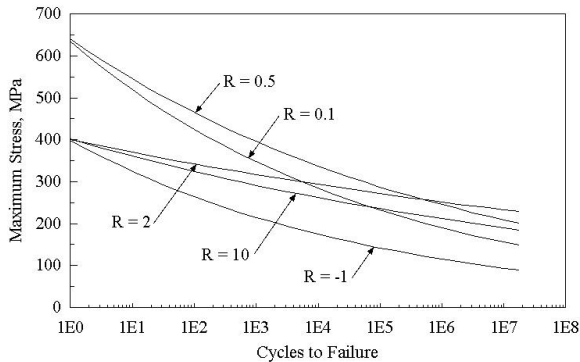


Figure 5. Laminate Constant Amplitude S-N Diagram Power Law Fatigue Model

Table I. Constant Amplitude Regression Constants

R-value	C_1	b	C_2	m
0.1	0.955	0.120	1.005	11.478
0.5	0.990	0.107	1.013	14.400
-1	0.994	0.125	0.998	11.158
10	0.994	0.081	1.005	21.550
2	1.000	0.062	1.000	29.820
UTS = 632 MPa, UCS = 400 MPa				

The constant amplitude data were also summarized into Goodman Diagrams (Figures 6 and 7) based upon the exponential and power law fatigue models

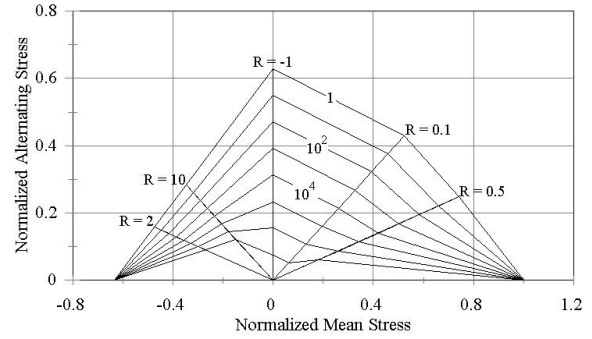


Figure 6. Laminate Goodman Diagram Based Upon Exponential Fatigue Models

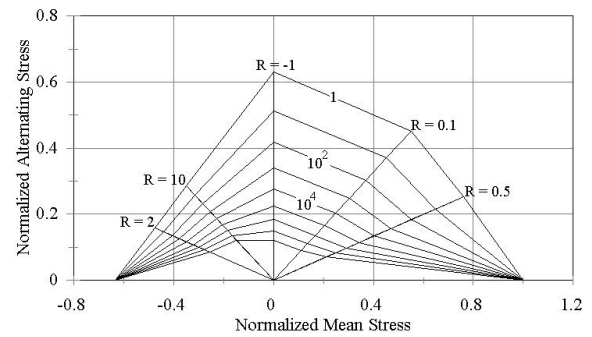


Figure 7. Laminate Goodman Diagram Based Upon Power Law Fatigue Models

Small Strand High Cycle Testing

The high cycle data for small strands were reduced to the S-N diagram of Figure 8. Also shown on this figure are the exponential and power law fatigue models. While better fits might be obtained by using different cycle ranges, the results in Figure 8 show a much better fit to the small strand data by the power law data, Equation 3, at high cycles. It should be noted that these results are for very small strands and show very high static strength compared with typical laminates [17]. The results are useful at the present time to clarify the choice of S-N models; data should not be used in design.

Multi-Block Testing

Block loading spectra with two, three and six different blocks of constant amplitude cyclic loads were used in fatigue testing of the selected laminate. Results for tension-tension testing were detailed in the previous report¹. Typical results for two-block tension-tension tests are shown in Figures 9 and 10. Miner's sum for the tests, are

shown related to the fractional amount of high amplitude cycles. These plots are shown with a split x-axis, with the extreme left margin displayed on a linear scale and the remainder on a logarithmic scale. This allows displaying the extremes of high amplitude cycle fractions. A fraction of 1 is the equivalent of a constant amplitude test at the higher maximum stress level; whereas, a fraction of 0 is a constant amplitude test at the lower maximum stress level. The average Miner's sums at these extremes are 1.0.

For cases such as that of Figure 9, where the stress levels are relatively far apart, there is a definite effect on the life and hence the Miner's sum. The trend is below a Miner's sum of 1.0 for high amplitude cycle fractions between 0 and 1.

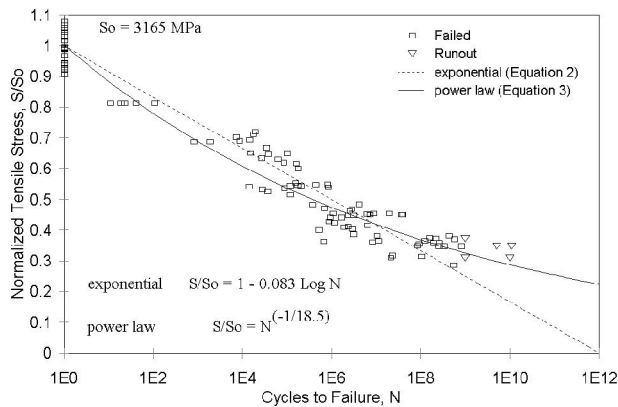


Figure 8. High Cycle/High Frequency Small Strand S-N Diagram (R=0.1) Exhibiting Exponential and Power Law Trends

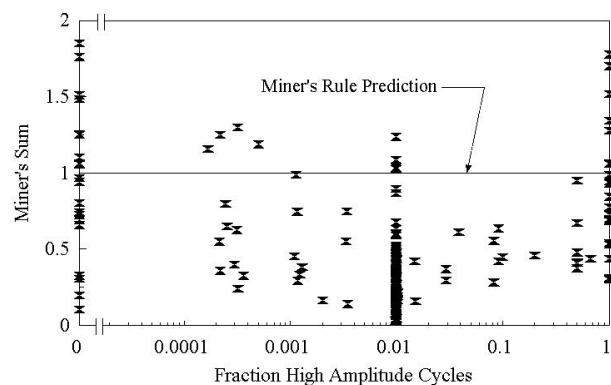


Figure 9. Two-Block Fatigue Trends With 325 and 207 MPa Maximum Stress Levels for the Two Blocks (R=0.1)

The limiting case of no difference between the stress levels of the two blocks would be a constant amplitude fatigue test at that common stress level. One would then expect that as the stress levels became closer, the degradation effect on the Miner's sum would become less. This is demonstrated in the example of Figure 10.

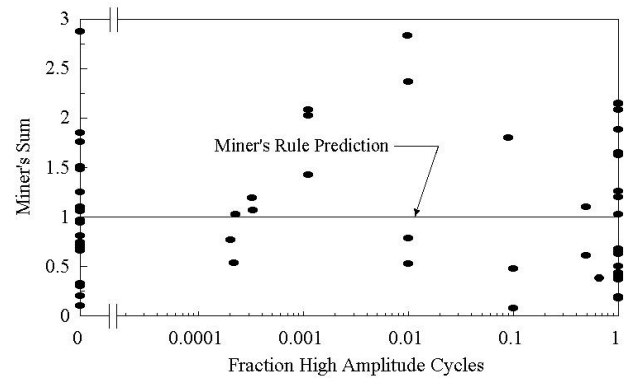


Figure 10. Two-Block Fatigue Trends With 235 and 207 MPa Maximum Stress Levels for the Two Blocks (R=0.1)

The compression-compression two-block fatigue tests do not exhibit depressed values of Miner's sums. Typical results for this type of testing are shown in Figure 11.

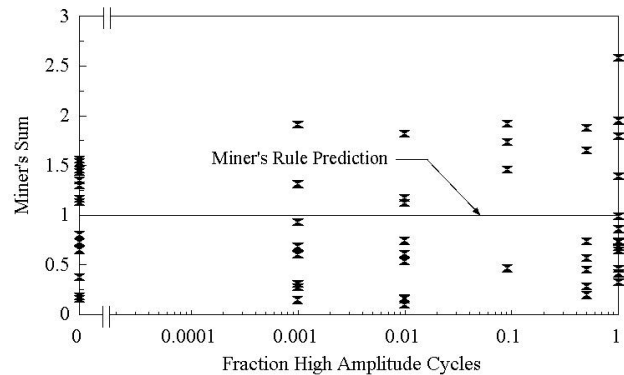


Figure 11. Two-Block Fatigue Trends With -275 and -207 MPa Minimum Stress Levels for the Two Blocks (R=10)

Fatigue testing under reversing load spectra do exhibit the characteristic reduced Miner's sum. Typical results for reversing two-block fatigue are shown in Figure 12.

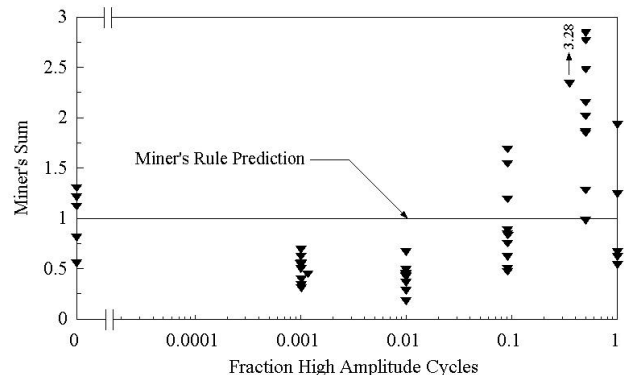


Figure 12. Two-Block Fatigue Trends With 173 and 104 MPa Maximum Stress Levels for the Two Blocks (R=-1)

The results of three and six block testing were reported in the previous paper¹. The Miner's sums for each of these repeated block tests were significantly less than 1.

Modified WISPERX Testing

Testing under a modified WISPERX spectrum was conducted as the next step in increasing the complexity of the spectrum. Fatigue results for one set of these tests (Mod 2 spectrum with a constant R-value of 0.1) have been summarized into the S-N diagram of Figure 13. The exponential and power law regression results are also displayed on this plot. The "slopes" for the two regression curves, b and m for the exponential and power law, respectively, are similar to the R-value of 0.1 constant amplitude values displayed in Table 1.

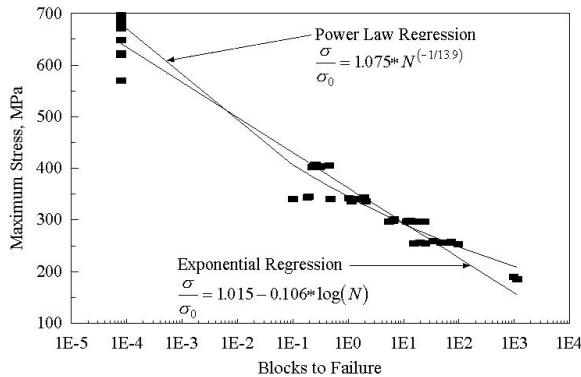


Figure 13. Mod 2 Spectrum S-N Diagram (R=0.1)

Unmodified WISPERX Testing

The original, unmodified WISPERX spectrum was also used to perform fatigue tests on the selected laminate. Results of these tests were reduced to the S-N diagram of Figure 14. Again, the regression results for exponential and power law fits are displayed in the plot. Little difference is found between the modified and unmodified WISPERX regression trends.

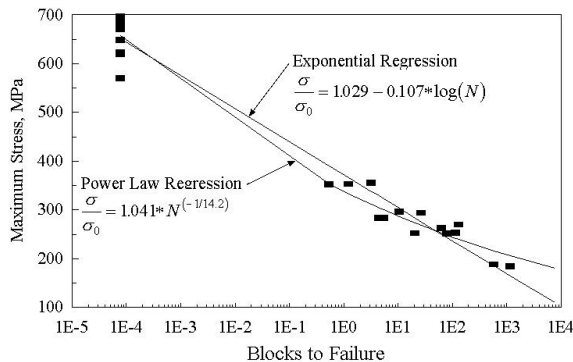


Figure 14. WISPERX Spectrum S-N Diagram

LIFETIME PREDICTIONS

Two-Block Spectra Lifetime Predictions

Lifetime predictions for the two-block cases reported earlier are shown in Figures 15 through 18. The Miner's rule prediction were shown in Figures 9 through 12. Residual strength degradation based predictions with a nonlinear degradation parameter of 0.265 are shown in Figures 15 - 18, based upon both the exponential and power law Goodman Diagrams of Figures 6 and 7, respectively. All prediction calculations were performed on a cycle-by-cycle basis. In each of the presented two-block cases, the exponential model provides a better correlation with the data than does the power law model at high values of the high amplitude fraction. The case shown in Figure 16, where the stress levels of the two blocks are relatively close, does not exhibit a significant difference between the exponential and power law fatigue models. The predictions cross at low high amplitude cycle fractions, and unfortunately, the choice of models is not readily determined from the data presented at the lower high amplitude cycle fractions. The lower fractions of high amplitude cycles are extending into regions of high total cycle counts, where a choice of the fatigue model may switch to the power law model.

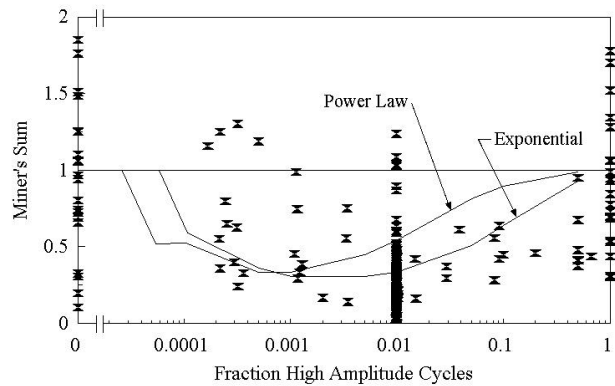


Figure 15. Lifetime Prediction for Two-Block Spectrum at 325/207 MPa Maximum Stress Levels (R=0.1); Exponential and Power Law Fatigue Models

Modified WISPERX Spectrum Lifetime Predictions

Lifetime predictions based upon both Miner's rule and a residual strength degradation based rule, for the Mod 2 WISPERX spectrum are shown in Figure 19. Regardless of whether the exponential or power law fatigue model is chosen (Goodman Diagrams of Figures 6 and 7) the Miner's rule is less conservative and predicts longer lifetimes than does the residual strength degradation rule. The power law

fatigue model does correlate better with the data than does the exponential fatigue model.

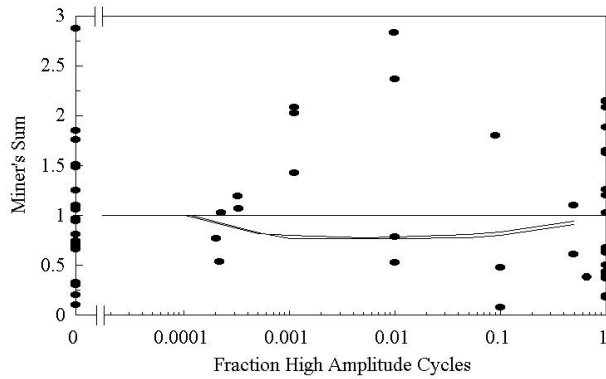


Figure 16. Lifetime Prediction for Two-Block Spectrum at 235/207 MPa Maximum Stress Levels (R=0.1) Employing Exponential and Power Law Fatigue Models

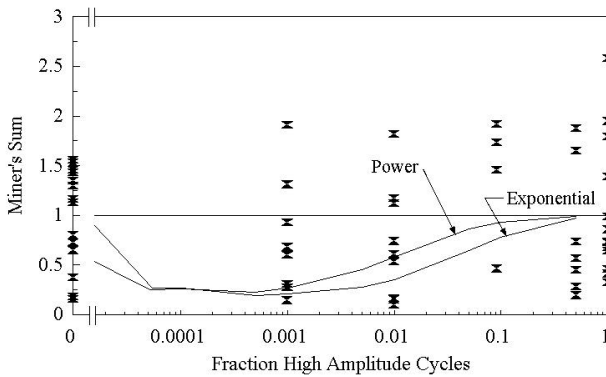


Figure 17. Lifetime Prediction for Two-Block Spectrum at -275/-207 MPa Minimum Stress Levels (R=10); Exponential and Power Law Fatigue Models

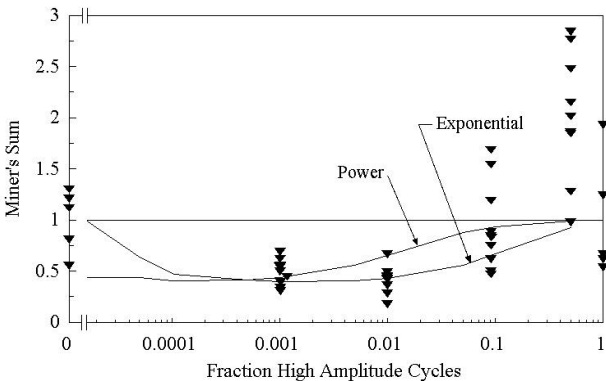


Figure 18. Lifetime Prediction for Two-Block Spectrum at 173/104 MPa Minimum Stress Levels (R=-1); Exponential and Power Law Fatigue Models

The predictions for less than one block of the

spectrum (less than one sweep through the spectrum) show discontinuities that are consistent with changes in the spectrum. These are mostly consistent with the one large event at approximately the 2500th cycle of the spectrum. The logarithmic scale hides this condition at the higher number of blocks to failure.

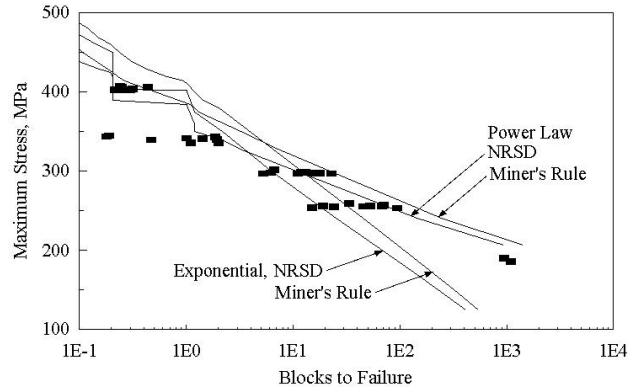


Figure 19. Lifetime Prediction for Mod 2 Spectrum (R=0.1); Exponential and Power Law Fatigue Models

Unmodified WISPERX Spectrum Lifetime Predictions

Predictions for laminate coupon lifetimes under the unmodified WISPERX spectrum are shown in Figure 20. The incremental stress magnitude for these predictions was coarse, consequently the discontinuities at the fractional block sizes are not as dramatic. The predictions based upon the power law fatigue model do follow the general trend of the data better than do the predictions based upon the exponential fatigue model. The power law provides non-conservative results as compared to the data, whereas the predictions based upon the exponential law pass through the data at a too-large slope, over-predicting life at the high stress levels and under-predicting life at the low stress levels.

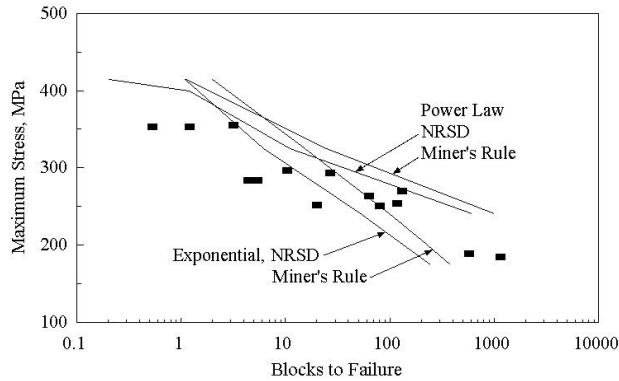


Figure 20. Lifetime Prediction for WISPERX Spectrum Employing Exponential and Power Law Fatigue Models

CONCLUSIONS

The selection of the fatigue model is dependent upon the relative number of cycles experienced. The two-block fatigue trends seem to indicate that the exponential fatigue model as represented by the Goodman Diagram, is more accurate than the power law model for the higher stress / lower cycle loading condition. Conversely, the results of the tests and predictions for the modified WISPERX spectrum clearly demonstrates that the power law provides a better correlation with the data, particularly at high cycles.

High cycle fatigue testing of tow coupons indicates that the general fatigue trend at the high cycles is better approximated by the power law fatigue model.

The method of handling the transition between tension and compression dominated failure for the residual strength degradation lifetime predictions needs refinement. Further details of this study may be found in Reference 18.

REFERENCES

1. Wahl, Neil, Samborsky, Daniel, Mandell, John, Cairns, Douglas, "Specrum Fatigue Lifetime and Residual Strength for Fiberglass Laminates in Tension," 2001 ASME Wind Energy Symposium, 39th AIAA Aerospace Sciences Meeting, Reno, NV, 2001, pp. 49-59.
2. ten Have, A. A., "WISPER and WISPERX, Final Definition of Two Standardised Fatigue Loading Sequences for Wind Turbine Blades," NLR TP 91476 U, National Aerospace Laboratory NLR, the Netherlands.
3. ten Have, A. A., "WISPER and WISPERX, A Summary Paper Describing Their Background, Derivation and Statistics," NLR TP 92410 U, National Aerospace Laboratory NLR, the Netherlands.

4. Miner, M. A., "Cumulative Damage in Fatigue," *Journal of Applied Mechanics*, Sept., 1945.
5. Sutherland, H. J., Mandell, J. F., "Application of the U.S. High Cycle Fatigue Data Base to wind Turbine Blade Lifetime Predictions," *Energy Week 1996*, ASME, 1996.
6. Sutherland, Herbert J., Veers, Paul S., Ashwill, Thomas D., "Fatigue Life Prediction for Wind Turbines: A Case Study on Loading Spectra and Parameter Sensitivity," *Case Studies for Fatigue Education*, ASTM STP 1250, Ralph I. Stephens, Ed., American Society for Testing and Materials, Philadelphia, 1994, pp. 174-207.
7. van Delft, D. R. V., de Winkel, G. D., and Joossee, P. A., "Fatigue Behaviour of Fibreglass Wind Turbine Blade Material Under Variable Amplitude Loading," *Proceedings of 35th Aerospace Sciences Meeting & Exhibit, 1997*, American Institute of Aeronautics and Astronautics.
8. Echtermeyer, A. T., Kensche, C., Bach, P., Poppen, M., Lilholt, H., Andersen, S. I., and Brøndsted, P., "Method to Predict Fatigue Lifetimes of GRP Wind Turbine Blades and Comparison With Experiment," *Proceedings of 1996 European Union Wind Energy Conference*, 1996.
9. Hwang, W. and Han, K. S., "Cumulative Damage Models and Multi-Stress Fatigue Prediction," *Journal of Composite Materials*, Vol. 20, 1986.
10. Yang, J. N. and Jones, D. L., "Effect of Load Sequence on the Statistical Fatigue of Composites," *AIAA Journal*, Vol. 18, No. 12, 1980.
11. Sutherland, Herbert J., "Damage Estimates for European and U.S. Sites Using the U.S. High-Cycle Fatigue Data Base," IEA R&D Wind Annex XI Symposium on wind Turbine Fatigue, DLR, Stuttgart, 1996.
12. Broutman, L. J. and Sahu, S., "A New Theory to Predict Cumulative Fatigue Damage in Fiberglass Reinforced Plastics," *Composite Materials: Testing and Design*, ASTM STP 497, American Society for Testing and Materials, 1972.
13. Schaff, Jeffery R. and Davidson, Barry D., "Life Prediction Methodology for Composite Structures. Part I - Constant Amplitude and Two-Stress Level Fatigue," *Journal of Composite Materials*, Vol. 31, No. 2., 1997.
14. Schaff, Jeffery R. and Davidson, Barry D., "Life Prediction Methodology for Composite Structures. Part II - Spectrum Fatigue," *Journal of Composite Materials*, Vol. 31, No. 2, 1997.
15. Samborsky, Daniel D., "Fatigue of E-Glass Fiber Reinforced Composite Materials and Substructures," Masters Thesis, Department of Civil Engineering, Montana State University, 1999, pp. 37-39.
16. Mandell, John F. and Samborsky, Daniel D., "DOE/MSU Composite Materials Fatigue Database: Test Methods, Materials, and Analysis," Contractor Report SAND97-3002, 1997.

17. Mandell, John F., Samborsky, Daniel D., Cairns, Douglas, C., and Wahl, Neil K. "Fatigue of Composite Materials and Substructures for Wind Turbine Blades," Contractor Report (to be published).

18. Wahl, Neil K., Mandell, John F. and Samborsky, Daniel D., "Spectrum Fatigue Lifetime and Residual Strength for Fiberglass Laminates," Contractor Report (to be published).